Journal of Archaeological Science 38 (2011) 233–245

Contents lists available at ScienceDirect

Journal of Archaeological Science

journal homepage: http://www.elsevier.com/locate/jas

The iron anchors from the Tantura F shipwreck: typological and metallurgical analyses

M. Eliyahu [a], O. Barkai [b], Y. Goren [c], N. Eliaz [a], Y. Kahanov [b], D. Ashkenazi [a,*]

[a] Faculty of Engineering, Tel Aviv University, Ramat Aviv 69978, Israel
[b] Leon Recanati Institute for Maritime Studies, University of Haifa, Haifa 31905, Israel
[c] Laboratory for Comparative Microarchaeology, Department of Archaeology and Ancient Near Eastern Civilizations, Tel Aviv University, Ramat Aviv 69978, Israel

ARTICLE INFO

Article history:
Received 10 March 2010
Received in revised form
18 August 2010
Accepted 21 August 2010

Keywords:
Ancient anchor
Archaeometallurgy
Blacksmith
Tantura F
Wrought iron

ABSTRACT

The *Tantura F* shipwreck was discovered in 1995 in Dor (Tantura) lagoon, about 70 m offshore. It was a coaster that plied the Levant coast during the local early Islamic period. Among the finds exposed in the wreck site were two iron anchors of the T-shaped type. This type of anchor, dated to between the second half of the fourth and the thirteenth centuries AD, is found throughout the Mediterranean. The anchors were analyzed by typological and archaeometallurgical methods, including radiography, metallographic cross-sections, microhardness tests, SEM/EDS analysis and Optical Emisson Spectroscopy (OES) analysis. Light microscopy revealed heterogeneous microstructure consisting of ferrite, Widmanstätten ferrite-pearlite or pearlite, which is typical of wrought iron made by bloomery. The metallographic and microhardness results revealed that decarburization had occurred, probably during the final hot-working process. The OES analysis, supported by SEM/EDS data, showed that the anchors are similar in composition. Soda-blast cleaning followed by chemical etching revealed the forge-welding lines, clarifying the manufacturing process, which is similar in the two anchors. Thus, it is likely that both anchors belonged to the same ship and, hence, were *in situ*. This information extends the limited knowledge of technologies and materials used, specifically for the development of metallurgy in the Eastern Mediterranean during the early Islamic period, and enlarges the database of the typology of anchors of that period.

1. Introduction

The *Tantura F* shipwreck is the remains of a small coaster that plied the Levant coast during the local early Islamic period. It was discovered in Dor (Tantura) lagoon (Fig. 1) in 1995, about 70 m offshore in about 1 m depth of water, under a sand layer mixed with shells and stones. The archaeological site spread over an area of 12 m × 4 m on the seabed, with a maximum depth of 2.5 m (Barkai and Kahanov, 2007: 21). Based on ^{14}C tests, some by accelerator mass spectrometry (AMS) of short-living organic materials, and ceramic typological analysis, the wreck was dated to between the mid-7th and the end of the 8th centuries AD, which is the local Early Islamic period (Barkai et al., 2010: 88–101). Among the finds exposed in the wreck site were two T-shaped iron anchors.

Although iron anchors are well known from the archaeological material culture throughout the Mediterranean, there is limited information concerning their characteristics and manufacturing process. Therefore, this study extends the typological information and enlightens the technological aspects of manufacturing the anchors, including the materials and processes used.

2. The anchors of *Tantura F*

Two iron anchors were found at the wreck site of the Tantura F: one on the starboard side and the other on the port side, close to the bow (Fig. 2). Both were found broken at the shank, with part of the shank and the anchor cable ring missing. Anchor A was found just under the hull, touching it (Fig. 3a), while Anchor B was found concreted to the outside of the planking below the hull (Fig. 3b). Both anchors were retrieved from the seabed covered by a 4 cm thick grey layer of encrustation and concretion composed of sea sand, shells and small stones. Anchor A was removed from the sea in the third excavation season (2006), while anchor B was retrieved during the fourth (2007). Once in the laboratory, optical macrographs and X-ray images were obtained, and the concretions were subsequently removed with minimum harm to the external layers of the anchors, which had been oxidized with the concretions. Despite the oxidation process, the metal remained in a good state of preservation.

* Corresponding author.
E-mail address: dana@eng.tau.ac.il (D. Ashkenazi).

0305-4403/$ – see front matter © 2010 Elsevier Ltd. All rights reserved.
doi:10.1016/j.jas.2010.08.023

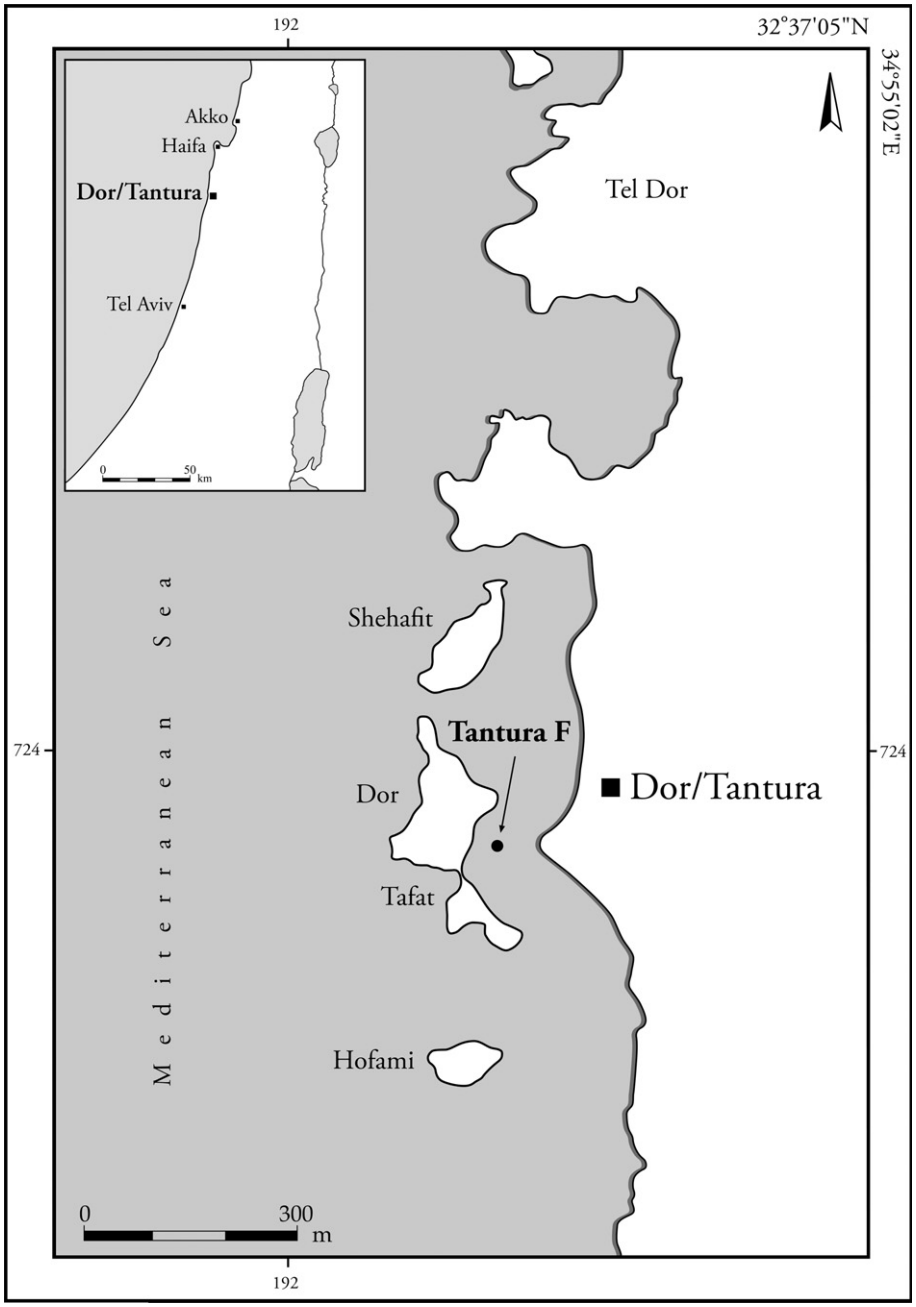

Fig. 1. Map of Dor.

The archaeological context and the maritime aspect of the wreck site raise some difficulties as to the anchors being *in situ*. The shipwreck was located southeast of Dor Island, as if the ship had almost been beached on the shore of the island. Anchors from other shipwrecks are expected to be found there; in fact, another shipwreck was discovered a few meters southeast of *Tantura F*. This was *Tantura B*, dated to the beginning of the 9th century AD (Wachsmann et al., 1997 [Trench XIII]). In the case of *Tantura F* the shanks were broken, and the cable rings missing, which makes it possible that the anchors did not belong to the shipwreck. Of the 68 anchors with shanks mentioned in the next section, 36 were discovered with broken shanks. The fracture zone always occurs at the weakest point of the objects, where maximum stress is present. The fractures of all 36 anchors, including those found with *Tantura F*, could have been a result of poor welding. It should be noted, however, that some of the anchors that were *in situ* were broken while others that were not *in situ* were found intact.

The connection of the anchors to the wreck of *Tantura F* is based on their location at the site, and partially on their typology, considering the date of the shipwreck. The anchors were under the ship, which rules out the possibility that they were dropped after the wrecking of *Tantura F*. If the anchors had been dropped by a vessel earlier than the *Tantura F*, they would probably have sunk deeper into the sand, as a result of the conditions inside the lagoon. The locations of the anchors, on both sides of the hull between frames F21 and F24, touching the timbers of the hull, as shown in Fig. 2, seem unlikely to have been a coincidence. A thick rope found under the ship may have been the ship's anchor cable. The metallurgical examinations (see below) show that both anchors have

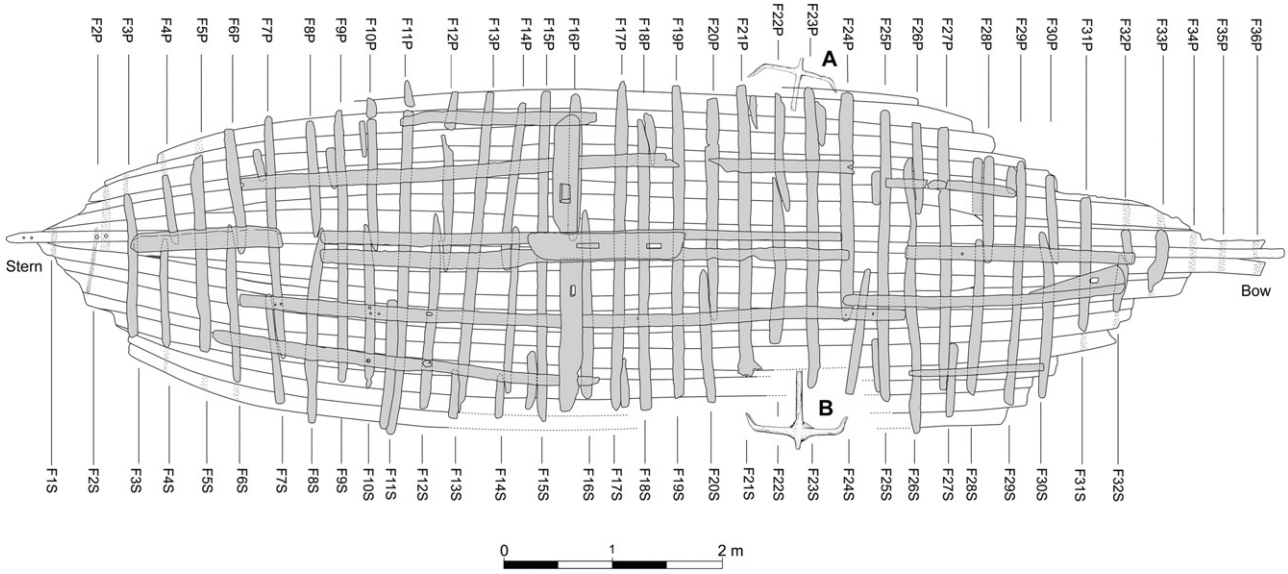

Fig. 2. Tantura F – top view with the anchors (C. Brandon and S. Haad).

a similar composition and manufacture process. Thus, it is very likely that the anchors belonged to the ship.

The anchors were T-shaped (see below) but the arms were not precisely perpendicular to the shank. The angles between the right and left arms and the shank, and the angles of the right and left tips relative to the arm in each anchor were not the same. This apparent distortion could have resulted from the forces imposed on the anchors in use. The cross-sections of both shanks are circular; although this is unusual for a wrought iron object, it is typical of T-shape iron anchors. The tips of the arms were flattened. The dimensions of both anchors after the removal of the external concretion layers are given in Fig. 4.

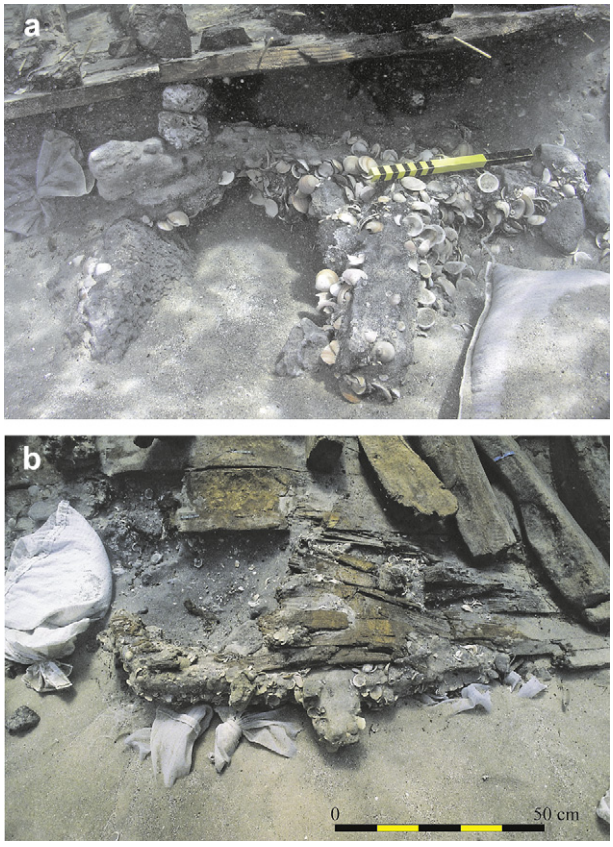

Fig. 3. (a) Anchor A beneath the planking (S. Breitstein), and (b) Anchor B attached to the vessel (I. Grinberg).

3. Anchors in late antiquity and medieval times

3.1. General

The purpose of the anchor is to hold a vessel in position in various conditions of water. A wide variety of anchor shapes and characteristics were developed, and they were used in combination with other measures, for example when mooring to a wharf. The anchor's shape was the result of technological knowledge, technical capabilities, and experience. The anchor requirements depended on the size of the vessel, type of anchorage, and nature of the ground (Kemp, 1976: 21).

The earliest forms of anchors were large stones that held a vessel by their weight only. In later periods, wooden flukes through the stone gripped the seabed. At the same time, the stone anchor developed into a two-armed wooden anchor with a perpendicular stone or lead-weighted stock. Iron anchors came into use in parallel with the use of wood and lead anchors; their shape was most probably adapted from that of the latter (Frost, 1963; Kapitän, 1984: 34, Fig. 2).

A typological-chronological analysis of iron anchors was made by Kapitän (Fig. 5), based on anchors discovered up to the 1980s (Kapitän, 1984: 42). In this classification, iron anchors were first used in the Roman Republican period, and were V-shaped with a rectangular stock. These anchors were similar in their shape to the wood and lead anchors, with the flukes of the anchors barely distinguishable. In the early Roman Imperial period, the arms were rounded with scarcely distinguishable tips and the stock was rectangular. In the later Roman Imperial period the arms were more horizontal and straightened, and the flukes were slightly raised, while the cross-section of the stock remained rectangular. At the end of the Late Roman period and during the local Byzantine and Islamic periods, T-shaped anchors were introduced: the arms were straight and at right angles to the shank, and the flukes were

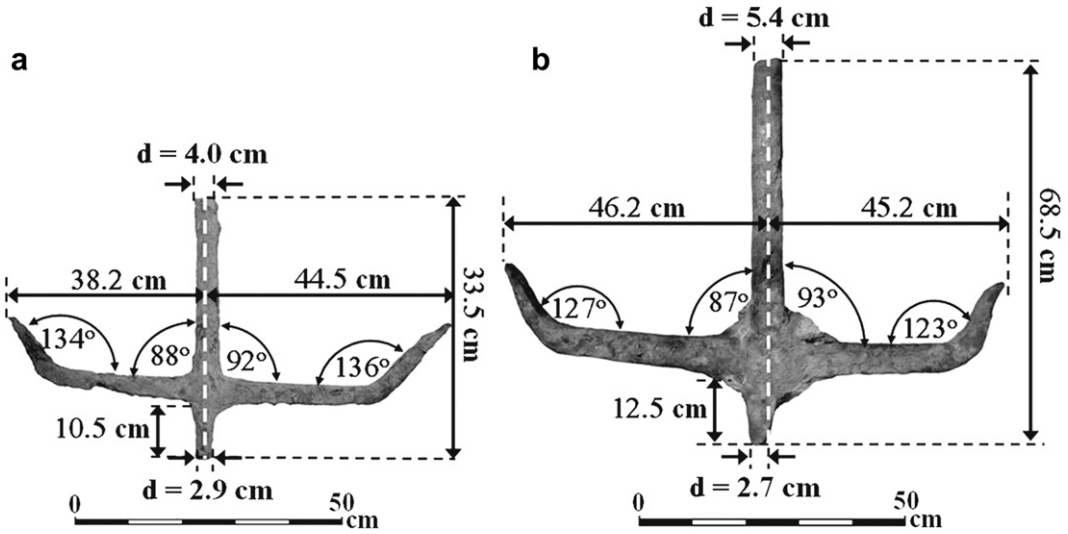

Fig. 4. (a) Measurements of the archaeological find Anchor A (front view), (b) measurements of the archaeological find Anchor B (front view).

inclined upwards, with the cross-section of the shank being circular. Later, Y-shaped anchors were introduced, as is evidenced by the anchors from the Serçe Limanı shipwreck, dated to AD 1025 (Van Doorninck, 2004: 189). Their arms inclined downwards at obtuse angles, and the flukes pointed upwards at right angles to the arms. In Kapitän's opinion, the obtuse angle of the arms of the Y-shaped anchors attests to a technological advance, as compared with the right angle found in the T-shaped anchors, since there was less chance that a Y-angled anchor would break, as there was less force on the connection points between the shank and the arms (Kapitän, 1978: 271). However Y-shaped anchors have been known from the 10th century as is evidenced by the anchors of Yenikapı 1 (Pulak, 2007: 132).

Haldane (1990: 22) suggested that the anchors of the Roman Imperial period, which are one type, C, in the typology of Kapitän, should be divided into two categories: the anchors of *Dramont D* (first century AD) being the earlier type, and those of *Dramont F* the later type.

3.2. T-shaped anchors

The earliest finds of T-shaped anchors from a dated archaeological context were excavated in the *Dramont F* shipwreck, which is dated to the second half of the 4th century AD. This anchor represents the transition phase from anchors with curved arms as were discovered in *Dramont D* and *Dramont F*, to T-shaped anchors. Four iron anchors were found in *Dramont F*: two had slightly curved arms—characteristic of an earlier type from the late Roman Imperial period, and two were T-shaped with short straight arms and straight flukes, which are bent slightly upwards (Joncheray, 1975: 116–118, 1977: 7). Later evidence of T-shaped anchors was found as is described in Table 1.

T-shaped anchors from undated archaeological contexts have been found on the island of Melita on the Dalmatian coast (Vrsalović, 1974: 138 Fig. 82, 83); Valencia, Spain (Martin and Saludes, 1966: LAM.IL:B); Cervia, Italy (Bonino, 1971: 320); Capo Graziano, Filicudi, Italy (Kapitän, 1978: 269); Sicily (Gargallo, 1961: 35, Fig. 11); Cilicia, Turkey (Marten, 2005: 59); Cape Andreas, Cyprus (Green, 1973: 168) and several in Israel: Haifa (Kapitän, 1969–1971: 54); Dor (Kingsley and Raveh, 1996: 23; Raveh and Kingsley, 1991:, 200); Netanya (observed by the authors, 2010); and Yavne Yam (Galili et al., 1993: 62).

In Kapitän's opinion (Kapitän, 1973: 385, 1978: 374), typological-chronological development can be noted in T-shaped anchors. The oldest T-shaped type seems to be a transition between the Roman and the Byzantine types. It was T-shaped with a stock of rectangular cross-section. Anchors of this type have been found near Yavne Yam (Galili et al., 1993: 62), Haifa and off the Spanish coast, but not in archaeological contexts (Kapitän, 1973: 385). The second type is represented by the early anchors from the *Dramont F* shipwreck, characterized by relatively short arms and long straight flukes which are only bent slightly upwards. The latest type is from the

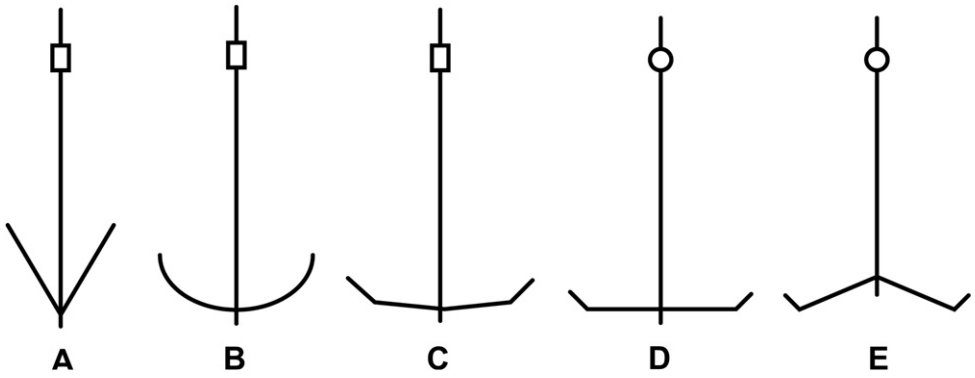

Fig. 5. A typological-chronological analysis of iron anchors made by Kapitän (1984).

Table 1
T-shaped anchors from dated archaeological contexts.

Place	Site	Quantity	Date (AD)	Reference
Black Sea port of Tomis, Romania	Store room	8	6th century	Canarache, 1967: 85
Sicilian coast	Shipwreck- *Cefalù*	1	6th–7th centuries	Purpura, 1983: 93–94
Turkey	Shipwreck-*Yassıada*	11	625/6	Van Doorninck 1982: 121
Seville, Spain		1	Second half of 6th century	Cabrera, 2007: 16–21
Dor (Tantura) lagoon, Israel	Shipwreck- *Dor J*	5	Between late 6th and early 7th century	Kingsley and Raveh, 1996: 60–61; Wachsmann and Raveh, 1980: 260
Turkey	Shipwreck- *Bozburun I*	2	874	Harpster, 2005: 5, 7; Hocker et al., 1998a: 13; Hocker et al., 1998b: 7–8
Southern coast of France	Shipwreck- *Agay A*	3[a]	Middle of the 10th century	Visquis, 1973: 158; Joncheray and Brandon, 2007: 226
Sea of Marmara, Turkey	Shipwreck-Çamaltiburnu	13[b]	13th century	Günsenin, 2005: 121

[a] Kapitän (1978: 271) defined them as Y-shaped, while Van Doorninck (1982: 234) proposed that they could have been T-shaped.
[b] Four broken Y-shaped and T-shaped anchors found together with an amphora assemblage dating to the 13th century AD, as well as 13 T-shaped anchors and 18 Y-shaped anchors found 17 m from the shipwreck. Despite this distance, the researcher believes that they comprised part of the cargo and belong to the same context (Günsenin, 2005: 121).

Yassiada shipwreck, which is characterized by longer arms with upward-curved flukes bent outwards. Common to the last two types is a round hole in the shank for a detachable stock. In the *Çamaltiburnu* shipwreck, which is dated to the 13th century, T-shaped anchors of different arm shapes were found in the same assemblage, but without evidence of the shape (round or square) of the stock, as this section of the anchor did not survive. Further evidence of T-shaped anchors appears in a church in Italy, dated to the same period (Bonino, 1971: 325). Anchors were used in Christianity as a symbol of the cross and of hope (Beckmann, 1967: 486); therefore, this cannot provide confirmation of the use of T-shaped anchors at that time.

Arms/shank ratio of different T-shaped anchors (Dramont F, Yassiada An.1, Yassiada An.3, Yassiada An.4, Yassiada An.5, Yassiada An.6, Yassiada An.7, Yassiada An.8, Yassiada An.9, Yassiada An.10, Yassiada An.11, Dor, Yavne Yam, Cervia, Tomis, Bozburun I, Cape Andreas) is summarized in Table 2, where arms (sum) is the distance between the two arm tips.

As at least part of the typological sequence is based on anchors which are out of archaeological context, it seems that further data and research are needed.

In summary, the use of T-shaped iron anchors was common throughout the Mediterranean, Marmara and Black Seas over a period of approximately 900 years, starting from the second half of the 4th century and lasting to the 13th century. At the beginning of this period, they were present in parallel to curved armed anchors, while from the 10th century they appeared together with Y-shaped anchors. However, it is difficult to establish a detailed typological development.

4. Background of the metallurgical analysis

At a relatively low temperature (800 °C), the reduction of iron is possible in the solid state, but only at about 1150 °C is the viscous slag capable of removing the unwanted gangue minerals of the ore (Tylecote, 1992: 46–57). This high temperature is not hot enough to melt iron with low carbon content, instead, the process produces a spongy mass called bloom, whose pores are filled with slag. After the reduction step, the bloom needs to be repeatedly hammered in order to remove the viscous slag and compact the metallic particles. This consolidation process, called primary forging, results in a nearly pure iron. In order to join two or more pieces of wrought iron made by the direct process, forge-welding is required. This is a hot-working process which requires a temperature below the melting point, T_m, usually $> 1/2\ T_m$ (Murray and Cliff, 1993: 156). At this temperature, the austenite phase is ductile and, hence, can be joined by hammering, following a solid-state diffusion under pressure mechanism.

Analysis of one sample anchor from the *Yassiada* shipwreck (Delwiche, 1982: 322) demonstrated that the anchor was forged.

Table 2
Shank/(arms sum) ratio of T-shaped anchors, where arms sum is the distance between tips.

Anchor	Distance between tips (m)	Length of shank (m)	Shank/(arms sum) ratio	Reference
Dramont F	0.68	1.40	2.06	(Joncheray, 1975: 118–9; 1977: 7 Fig. 8)
Yassiada An.1	1.41	2.14	1.52	Van Doorninck, 1982: 125,126 Figs. 6–12
Yassiada An.3	1.29	2.19	1.70	Van Doorninck, 1982: 125, 127 Figs. 6–14
Yassiada An.4	1.58	2.04	1.29	Van Doorninck, 1982: 125, 128 Figs. 6–15
Yassiada An.5	1.53	2.38	1.56	Van Doorninck, 1982: 125, 128 Figs. 6–16
Yassiada An.6	1.42	2.57	1.81	Van Doorninck, 1982: 126, 129 Figs. 6–17
Yassiada An.7	1.35	2.25	1.67	Van Doorninck, 1982: 126, 129 Fig. 6: 18
Yassiada An.8	1.57	2.47	1.57	Van Doorninck, 1982: 126, 129 Figs. 6–19
Yassiada An.9	1.54	2.00	1.30	Van Doorninck, 1982: 126, 130 Figs. 6–20
Yassiada An.10	1.50	2.41	1.60	Van Doorninck, 1982: 126, 131 Figs. 6–21
Yassiada An.11	1.55	2.42	1.56	Van Doorninck, 1982: 127, 131 Figs. 6–22
Dor	0.4	0.75	1.88	Kingsley and Raveh, 1996, 23, pl. 18 MA12; Kingsley and Raveh, 1996: Figs. 20–22: MA12
Yavne Yam	0.85	1.50	1.77	Observed in the National Maritime museum in Haifa
Yavne Yam	0.97	1.85	1.91	
Cervia	0.69	1.14	1.65	Bonino, 1971: 320, fig. 4
Tomis	–	–	1.39	Canarache, 1967: 85
Tomis	–	–	1.44	
Tomis	–	–	1.55	
Bozburun I	–	–	1.71	Hocker et al., 1998a: 13, Fig. 2
Cape Andreas	–	–	1.65	Green, 1973: 168

Although the exact number of forge-welded pieces is difficult to determine, it is suggested that "there were 4 pieces in either arm and perhaps as many as10 pieces in the shank" (Van Doorninck, 1984: 3–7). The material was almost clear of slag, with a carbon content of 0.07 wt.%, with irregularly shaped grains in a wide size range. The other elements in the anchor material, aside from iron (all elements were analyzed by wet chemical and spectrographic analysis), were potassium (0.06 wt.%), sulphur (0.008 wt.%), silicon (0.14 wt.%), sodium (0.005 wt.%), magnesium (0.005 wt.%), aluminium (0.05 wt.%), calcium (0.005 wt.%), titanium (0.005 wt.%), vanadium (0.01 wt.%), chromium (0.1 wt.%), manganese (0.007 wt.%), cobalt (1.0 wt.%), nickel (0.5 wt.%), copper (0.005 wt.%), zirconium (0.5 wt.%) and silver (0.0005 wt.%). The forging of the anchor was carried out at a temperature of about 1100–1150 °C. The location at which the iron was smelted was not identified (Delwiche, 1982: 322–324). This manufacturing method was also used to produce Y-shaped anchors, as in the anchors from Serçe Limanı. These anchors weighed between 47.5 and 67.4 kg, and were made of 17 forged pieces (including the ring) which were forged together, each weighing between 4 and 5 kg (Stech and Maddin, 2004:, 193).

Recent archaeometallurgical studies (Stech and Maddin, 2004:193, Kocabaş, 2009: 227–237) demonstrate clearly that artifacts such as anchors are made by forge welding of different semi-products, which have been obtained from different consolidated blooms. The goal of the present investigation is to answer questions such as how many blooms were used and what the welding operations to produce the anchor were. Since little information is available in the literature about the manufacturing processes of iron anchors in the in the Late Antique and early Medieval period, during which no hydraulic hammers were was used to form wrought iron, this article presents useful information about these kinds of large artifacts, clarifying questions such as whether both anchors were manufactured in the same workshop and whether the same raw material was used in both smelting processes.

5. Experimental methods and tests

Both anchors were analyzed by their typology and by archaeometallurgical methods, including: radiography, metallurgical optical microscope (OM), Vickers microhardness test, SEM/EDS analysis and OES chemical analysis, as shown in Table 3.

Three metallographic cross-sections, marked F, G and H, were taken from two different zones of Anchors A and B. These sections were perpendicular to axes z, x and y, respectively, as suggested by ASTM E3-01 and shown in Fig. 6. In order to cause minimal damage to both anchors, the metallographic samples were cut from only two cylindrical slices. The first slice was cut from the top of the shank (Zone a), while the second slice was cut and pulled out from the joint area (Zone b). From the first slice, 4 samples were cut – two parallel F sections (from both side of the slice, along the entire diameter), one G section, and one H section. From the second slice, 5 samples were cut – three parallel H sections (from different depths along the extruded drilled cylinder), one F section, and one G section. The samples were cut with a water-cooled steel disc and then hot-mounted in Bakelite (at a temperature of 180 °C and pressure of 180 psi). The preparation of the surface consisted of grinding with silicon carbide papers (240–600 grit), then polishing with alumina paste from 5 to 0.05 μm, and finally polishing with 0.05 μm colloidal silica suspension pastes. The samples were cleaned in an ultrasonic bath to remove any contaminants, then cleaned with ethanol and dried. They were then etched using Nital (97 mL ethyl alcohol and 3 mL nitric acid). The metallographic samples were examined under an OM (ZEISS, AXIO-Scope A.1) up to ×1000 magnification. Vickers microhardness tests were performed along the diameter of the slice cut from the shanks of both anchors (Section F, Zone a), using a load of 100 g-force (gf). Measurements were conducted at 0.5 mm intervals using a Future-Tech Model FM-700e microhardness tester.

Chemical analysis was performed using the Optical Emission Spectroscopy (OES) (Pollard et al., 2007) technique with a Spectrolab Model M instrument, which has a detection limit <1%. Each sample area analyzed was 1×1 cm^2. The surface of the sample was ground and cleaned in an ultrasonic bath prior to this test. Two clean samples per anchor were analyzed.

SEM examination was performed in combination with EDS analysis. Imaging was done with a FEI Quanta 200FEG Environmental Scanning Electron Microscope (ESEM), under high vacuum mode, using the Everhart-Thonley secondary electron (SE) detector. Several zones with different surface morphologies were characterized. The chemical elemental composition was determined locally by energy dispersive spectroscopy (EDS) using Si(Li) liquid-cooled Oxford X-ray detector.

Non-destructive testing (NDT), namely radiography, was performed on both anchors using X-ray radiation, Eresco 200 machine, 200 kV, 4.5 mA, with 5–12 min of exposure time, on D7 Agfa film. Finally, the samples were cleaned by soda-blasting and then chemically etched in Nital to reveal the forge-welding lines.

6. Results

6.1. Reconstruction of the original dimensions and weights of the anchors of Tantura F

A reconstruction of the anchors from *Tantura F* was achieved by comparing the ratio between the dimensions of the arms and the shanks in twenty similar T-shaped iron anchors shown in Table 2. The average shank/(arms sum) ratio for these specimens is 1.63 ± 0.19. The original weights of both anchors were calculated by multiplying the volume of the reconstructed shanks by the density

Table 3
The scientific methods used in the present study.

Object	Location	Description	Testing methods					
			Radiography	Soda Blasting & Etching	OM	HV	SEM & EDS	OES
Anchor A	In the starboard between frames F21 and F24, touching the timbers of the hull.	Covered with concretion and with broken shank.	+After removing the concretion (7 measurements).	+	+9 metallographic samples.	+	+	+
Anchor B	In the port side between frames F21 and F24, touching the timbers of the hull.	Covered with concretion and with broken shank.	+Before removing the concretion (5 measurements) and (7 measurements) after removing the concretion.	+	+9 metallographic samples.	+	+	+

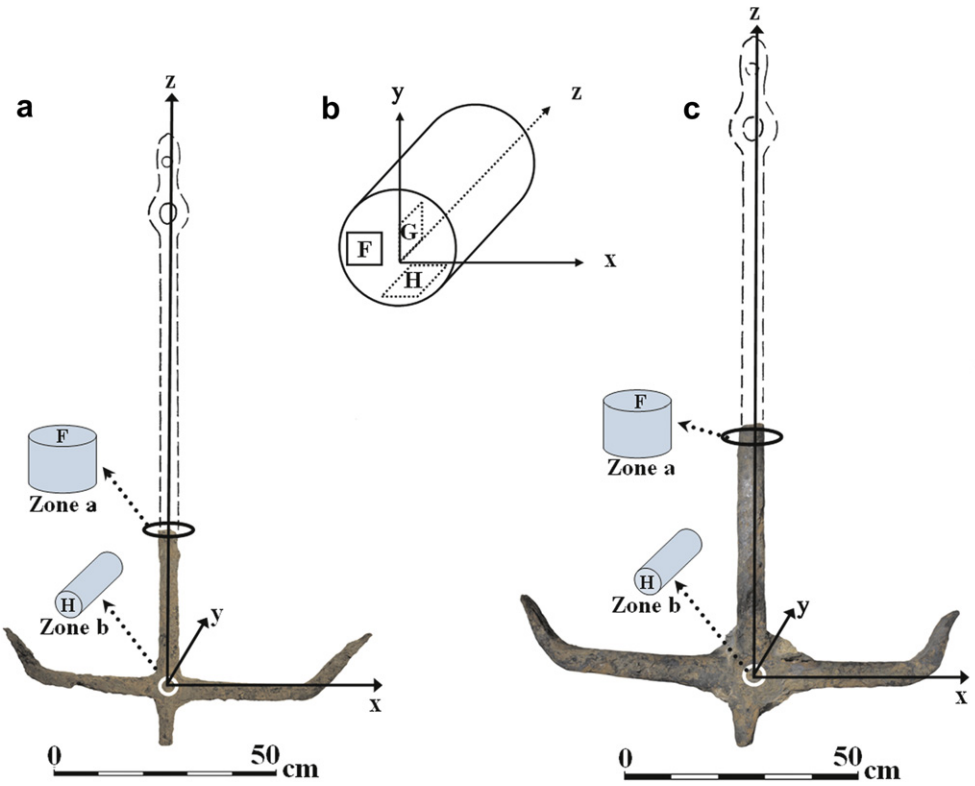

Fig. 6. (a) Reconstruction of Anchor A, with the location of the sampling on the anchor (Zones a and b), (b) reconstruction of Anchor B, with the location of the sampling on the anchor (Zones a and b), (c) the three metallographic cross-sections: F transverse section, G radial longitudinal section (perpendicular to the rolled surface), and H tangential longitudinal section.

of pure iron (ρ = 7.8 g/cm^3), since larger error is caused by the measurements of the anchor volume than by the variation of iron density caused by minor elements. Considering the good state of preservation, the calculation of the volume is based on the existing metal remains, ignoring loss due to corrosion. The estimated lengths were calculated by multiplying the average arm/shank ratio by the measured length of both arms (Fig. 6). The error of the measured values is negligible. The estimated weights were calculated using the following equation: $W_{\mathrm{rec}} = \rho \cdot \pi \cdot (d/2)^2 \cdot (L_{\mathrm{rec}} - L_{an}) + W_{an}$, where W_{rec} is the reconstructed weight, ρ is the density of pure iron, d is the diameter of the shank, L_{an} is the anchor (artifact) length, L_{rec} is the reconstructed length, and W_{an} is the anchor (artifact) weight.

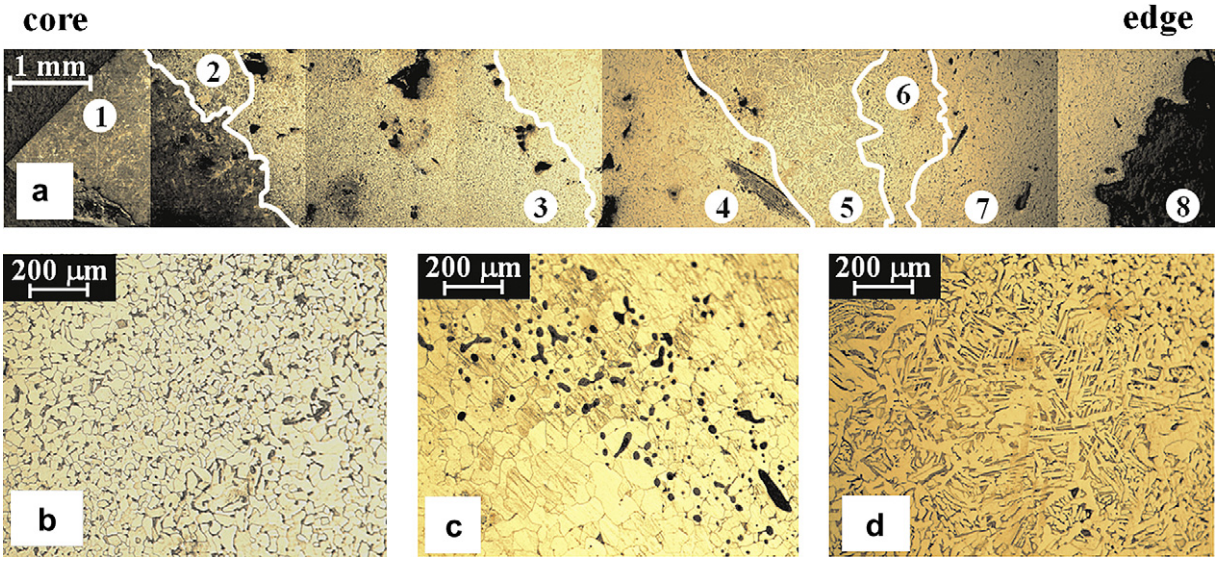

Fig. 7. (a) Light microscopy panorama metallographic image of Anchor A, Zone a, Section F (along the radius of the sunk), revealing a heterogeneous microstructure: Area 1 shows large pearlite grains, Area 2 shows pearlite matrix with Widmanstätten ferrite, Areas 3 and 6 show fine ferrite grains with pearlite at grain boundaries, Areas 4 and 7 show large ferrite grains, Area 5 shows Widmanstätten ferrite growth and pearlite phase, and Area 8 shows a corroded area, (b) Higher magnification of zone 3, (c) higher magnification of Area 4, (d) higher magnification of Area 5.

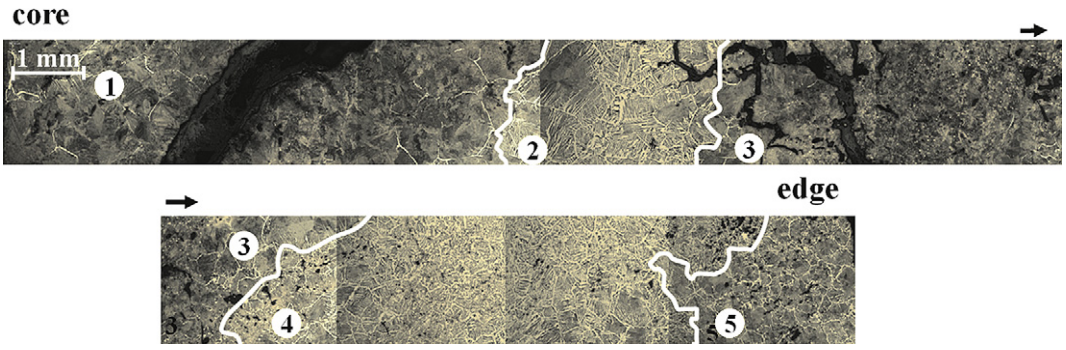

Fig. 8. Light microscopy panorama metallographic image of Anchor B, Zone a, Section F (along the radius of the shank), revealing a heterogeneous microstructure, with large pearlite grains with a small amount of Widmanstätten ferrite, as shown in Areas 1, 3 and 5 and Widmanstätten ferrite growth with pearlite phase, as shown in Areas 2 and 4.

The estimated lengths and weights for the reconstructed Anchor A are 134.9 ± 15.9 cm and 20.4 ± 1.6 kg, respectively, and for Anchor B: 152.8 ± 18.0 cm and 35.7 ± 3.2 kg.

6.2. Metallurgical analysis

Observation of the metallographic samples of Section F, from Zone a (in both anchors), from the core to the edge of the specimen, using ×50 magnification, revealed a heterogeneous microstructure relatively pure of slag inclusions and porosity, with only 3.4 area% of inclusions present for the measured surface of anchor A (Fig. 7) and 4.8% inclusions for the measured surface of anchor B (Fig. 8). The repetitiveness of these results was clarified, for both anchors, from both sides (upper and lower) of the cylindrical slices (cut from Zone a). Observation in sections G and H showed an equiaxed grain structure in both anchors. This result is expected, because oriented grain structure may be expected in these sections if force was applied in the *z*-direction, which is not reasonable unless this kind of force was used for lap-joint welding of the reconstructed shank to the artifact. Nevertheless, forge welding might not leave orientation traces because the temperature needed for this process is sufficient for recrystallization. Fig. 7a shows eight areas of different microstructures starting with pure pearlite at the core (Area 1), then pearlite matrix with Widmanstätten (thin plates or lamellas) ferrite (Area 2), fine ferrite grains with pearlite at grain boundaries (Area 3), large ferrite grains (Area 4), Widmanstätten ferrite growth and pearlite phase (Area 5), fine ferrite (Area 6), large ferrite grains (Area 7) and finally the corrosion layer (Area 8). Small cracks and pores are evident. Fig. 7b shows a higher magnification of Area 3, emphasizing the variety in grain size, typical of hand-forged iron (Delwiche, 1982: 323). Fig. 7c shows Area 4, associated with slag inclusions lightly oriented, whereas Fig. 7d shows a higher magnification of Area 5. Fig. 8 shows five areas of different microstructures, in the following order: large pearlite grains with a small amount of Widmanstätten ferrite at the core, Widmanstätten ferrite growth and pearlite phase, large pearlite grains with a small amount of Widmanstätten ferrite, Widmanstätten ferrite growth and pearlite phase, and large pearlite grains with a small amount of Widmanstätten ferrite. Slag inclusions, cracks and pores are shown in Fig. 8. An equiaxed grain structure is seen in all three sections of Zone b in both Anchor A (Fig. 9a for section F; Fig. 9b for section G; and Fig. 9c for section H) and Anchor B (Fig. 10a for section F; Fig. 10b for section G; and Fig. 10c for section H), meaning that the anchors were hot-worked, followed by recrystallization of the metallic grains in the forge-welding process. In Zone b, sections F and G are expected to present oriented grain structure if a force was applied in the *y*-direction, which is reasonable in the case of welding the shank to the arms, but again only in a cold-work process. The other two parallel H sections showed the same results in both anchors. In addition, the metallographic images shown in Figs. 9 and 10 are almost 100% free of slag inclusions and porosity suggesting that this area (Zone b), in both anchors was well hammered, probably during the forge-welding process.

Vickers microhardness values acquired in Anchors A and B are presented in Figs. 11a and 12a, respectively. Because it is obvious from Figs. 7 and 8 that the core of the shank of both anchors contain the largest amount of a pearlite phase, which decreases at the edges (a repetition of this result was assured for both anchors, as previously mentioned), an attempt was made to present those decarburization profiles, using microhardness data, while assuming that the hardness was mostly affected by the chemical composition (particularly for iron with low contents of other elements and a uniform mechanical and heat treatment history). In addition, when inclusions or corrosion products appeared along the diameter line, the microhardness test was conducted in a separate area nearby. For this purpose a linear calibration function (using least-square fitting) was employed for each anchor, describing the microhardness test results as a function of the carbon weight percentage, according to the lever rule in hypoeutectic steel. In order to obtain the calibration function, Vickers microhardness

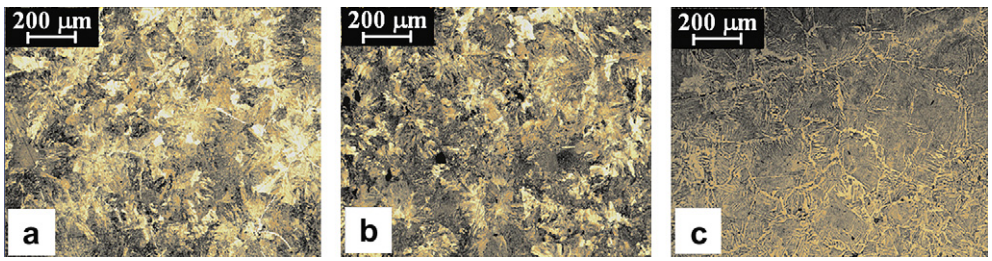

Fig. 9. Light microscope images from Zone b of Anchor A, showing an equiaxed grain structure. (a) from Section F and (b) from Section G show coarse pearlite and Widmanstätten ferrite, (c) from Section H shows mostly pearlite phase.

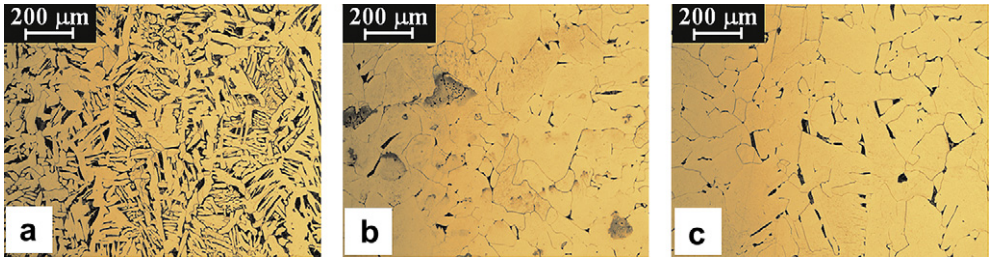

Fig. 10. Light microscope images from Zone b of Anchor B show no equiaxed grain structure. (a) Section F shows Widmanstätten ferrite growth and pearlite phase. (b) from Section G and (c) from Section H show ferrite grains with small amount of pearlite at grain boundaries.

tests were made in areas of either pure ferrite or pure pearlite in both anchors. The corresponding values were 128 ± 5 VHN (ferrite) and 332 ± 10 VHN (pearlite) for Anchor A; 106 ± 7 VHN (ferrite) and 292 ± 18 VHN (pearlite) for Anchor B. The microhardness values as a function of the distance were substituted into the calibration function in order to obtain the carbon wt.% as a function of distance. The results are shown in Figs. 11b and 12b, for Anchors A and B, respectively.

The results of the chemical analysis (OES) are shown in Table 4. Their relation to the analysis of the T-shaped iron anchor from *Yassiada* is discussed in the next section. Moreover, in order to better determine whether both anchors were manufactured, from the same ore, SEM images and EDS analysis of typical slag inclusions were acquired for both anchors, Zones a, section F (Fig. 13 and Table 5). Since there is very little phosphorus in the samples, as shown in Table 4, the iron is likely to be purely ferritic and a bog ore was probably used in the manufacturing. Fig. 13 shows an identical morphology of both slag inclusions. This morphology is typical of wüstite (FeO) trapped in a glassy matrix (Buchwald and Wivel, 1998:75).

Since no forge-welding lines were observed in the radiography test, we searched for forge weld trace lines at the surface. Soda-blast cleaning followed by chemical etching revealed the forge-welding lines, as shown in Fig. 14. It should be mentioned that while these macro observations were made on the entire anchors, we present here only the area in which forge-welding lines did appear. This approach has made it possible to suggest an interpretation for the manufacturing process of the anchors.

7. Discussion

7.1. The metallurgical aspect

The heterogeneous microstructure of almost pure ferrite through Widmanstätten ferrite and Widmanstätten ferrite-pearlite to pure pearlite shown in Figs. 7 and 8 is a result of high separation in the carbon content, and is typical of wrought iron made in ancient bloomeries (Buchwald, 2005: 296; Friede, 1979: 372; Tylecote, 1968; Stech and Maddin, 2004:, 192). This heterogeneous microstructure probably results from the heterogeneous conditions inside the furnace (temperature, gas concentration, etc.)

All slag inclusions observed in all the metallographic samples of Anchors A and B, Zones a and b, sections F, G, H (as shown, for example, in Fig. 7c), were in very low concentration, compared to wrought iron made in ancient bloomeries (Dillmann and L'Héritier, 2007: 1810). This fact, which will be further supported by the chemical analysis, is evidence of a highly skilled blacksmith. The slag inclusions located in section F (Fig. 7a) are relatively equiaxed since a relatively isostatic force was applied on the rod during consolidation.

The carbon-rich areas present in all of the metallurgical samples could be the result of natural carburization at relatively high

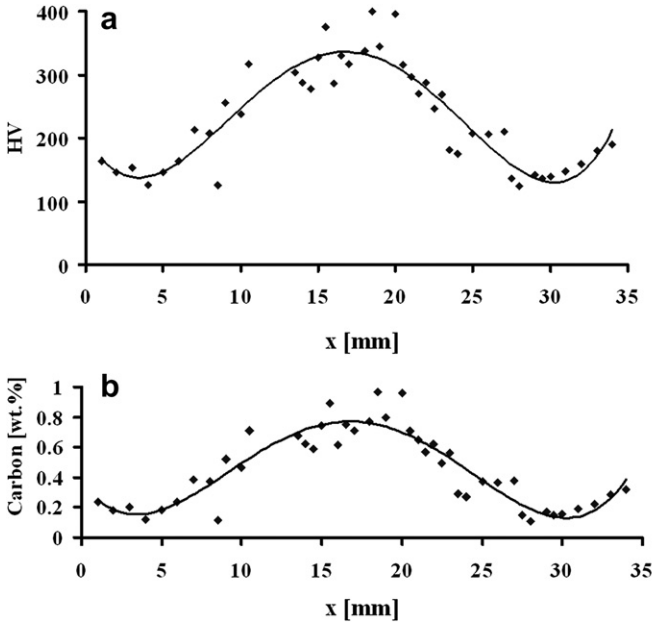

Fig. 11. (a) Vickers microhardness (m = 100 gf) along the x-axis on the diameter of the shank, Anchor A, Zone a, Section F, and (b) carbon weight percent *vs.* distance along the diameter of the shank, Anchor A, Zone a, Section F.

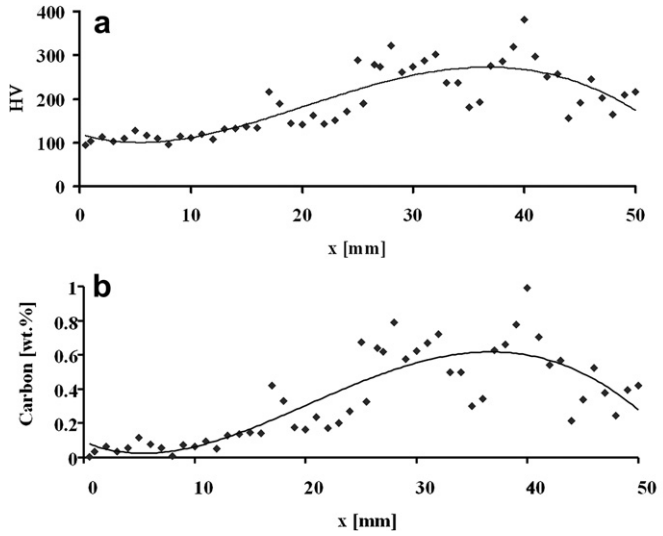

Fig. 12. (a) Vickers microhardness (m = 100 gf), along the x-axis, on the diameter of the shank, Anchor B, Zone a, Section F, and (b) carbon weight percent *vs.* distance along the diameter of the shank, Anchor B, Zone a, Section F.

Table 4
Chemical analysis (by OES) of both anchors, both in zone a and zone b. The results are presented in wt.%.

	C	Fe	Cu	Mo	Ni	Cr	S	P	Mn	Si	Fe
Anchor B Zone a	0.23	99.4	0.004	0.002	0.012	0.004	0.005	0.005	0.021	0.064	99.4
Anchor A Zone b	0.13	99.7	0.017	0.001	0.016	–	0.008	0.025	0.004	0.004	99.7
Anchor B Zone b	0.61	99.2	0.002	0.001	<0.001	–	0.003	0.007	0.037	0.029	99.2
Anchor A Zone a	0.41	99.2	0.005	0.001	0.054	–	0.005	0.074	0.004	0.088	99.2

temperatures and the strong reducing power of the CO/CO_2 gas. This could have occurred either in the smelting step, when carbon was absorbed and diffused into the reduced iron from the hot charcoal bed, or by absorption and diffusion into the metal close to the tuyères; or in the forging step, when it was trapped in the pores of the bloom when the slags were hammered out (Friede, 1979: 372). The presence of a Widmanstätten ferrite structure is an indication of prolonged heating of the austenitic phase and rapid air-cooling (Garagnani et al., 1996: 83; Bhadeshia, 1985: 321). From Fig. 11b it is clearly evident that a decarburization process had probably occurred during prolonged heating before forge-welding.

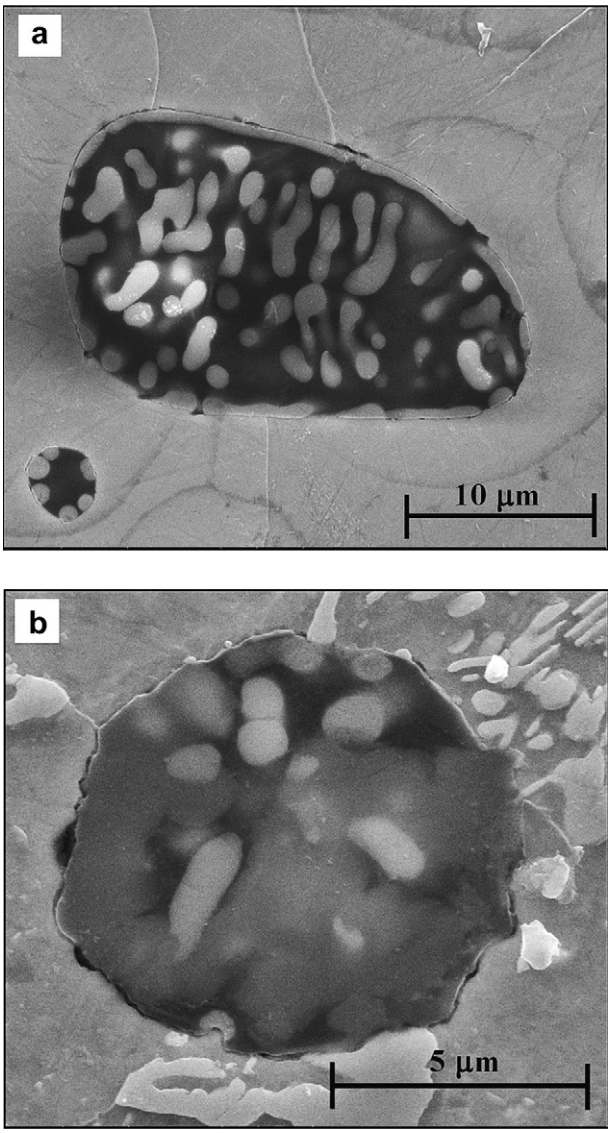

Fig. 13. SEM images of typical slag inclusions: (a) Anchor A, Zone a, Section F, and (b) Anchor B, Zone a, Section F.

From Fig. 12b it is also apparent that a decarburization process had occurred, although not a uniform one.

The chemical analysis presented in Table 4 supports the metallurgical observation that both anchors contain a larger amount of carbon than wrought iron made in ancient bloomeries, and especially with respect to the T-shaped iron anchor from the *Yassiada* shipwreck (0.07%). The low content of manganese indicates that no deliberate attempt was made to harden the iron by adding a manganese ore to the furnace. The purity of the iron is clearly very high, indicating high quality manufacturing. The similar chemical compositions of the two anchors, compared with those of the *Yassiada* shipwreck, suggest that the *Tantura F* anchors were made in the same type of furnace. From Table 4 it is clear that both inclusions have the same minor elements, except for phosphorous that appears in the inclusions from Anchor A only. Because an analysis of minor and trace elements present in individual inclusions should reflect the elements present in the original ore, it is very likely that the same process and ore were used for the manufacturing of both anchors. Nevertheless, in order to compare the origin of both anchors in a more profound way, an extended element slag inclusion study is necessary, like the work of Dillmann and L'Heritier (2007) and Blakelock et al. (2009). Further metallographic examination, including more sections on both anchors, will be done in the future, but only after performing radiographic CT analyses to both anchors. That, however, is beyond the scope of this paper.

7.2. Reconstruction of the manufacture of ancient iron anchors

The quality of forge welds is much dependent on the blacksmith's skills, since, at the working temperature mentioned, iron oxides are readily formed on the surface and their presence decreases the weld strength. So their formation should be prevented in advance. This can be done by welding two bloom pieces during their own consolidation, while removing the slag. In this process, welding lines are not expected to be seen at all. Another option is to remove the oxide film mechanically before hammering the two shaped pieces, or by using flux. In the later process, forge-welding lines are expected to be noticeable only as iron oxide inclusions (without any glassy phases) in the case of mechanical cleaning, or as iron oxide inclusions including glassy phases or at least silicate phases in the case of using flux. Nevertheless, the probability of locating them in radiography or in OM is highly

Table 5
EDS measured analysis of typical slag inclusions from Anchor A, Zone a, Section F (Fig. 13a), and from Anchor B, Zone a, Section F (Fig. 13b).

Element [wt.%]	Typical inclusion [Anchor A]	Typical inclusion [Anchor B]
O	13.86	24.46
Al	2.43	1.15
Si	9.76	5.2
P	1.20	–
K	1.28	0.93
Ca	17.06	2.89
Mn	2.00	1.98
Fe	52.37	61.4

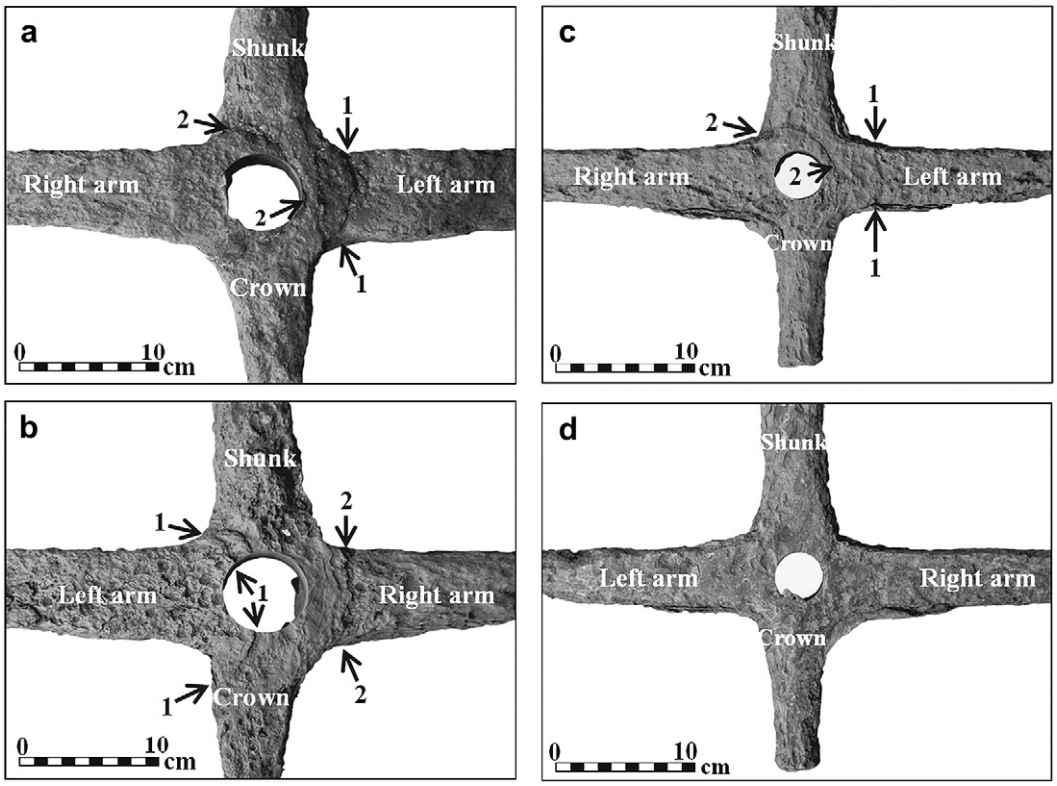

Fig. 14. Exposed forge-weld lines, after removing the corrosion layer with soda blasting and etching one side (front for Anchor B and back for Anchor A) of each anchor. a – back of Anchor B, b – front of Anchor B, c – back of Anchor A, d – front of Anchor A.

dependent on the quality of the work. Poor forge welds are expected to break under relatively low force, as in the case of the Serçe Limanı anchors (Stech and Maddin, 2004: 193). A very poor weld quality could probably be detected by radiography, since the density of the oxides is much lower than that of iron. Then, a black line would appear in the radiography film (similar to fracture), as in the case of the *Çamaltiburnu* shipwreck (Kocabaş, 2009: 227–237). A good forge weld might leave recrystallized ferrite or pearlite grains with very few iron oxide inclusions and very few voids (Murray and Cliff, 1993: 156). Hence, it might not be easily observed, surely not by radiography, but neither by OM nor by SEM. As in the present case, it may only be evident on the metal surface, enhanced through slightly etching. Since the radiography images showed no sign of welding lines in Zones B of both anchors, and since the representative metallographic images from Figs. 9 and 10 showed no forge-welding lines, and no unique amount of oxide or glassy inclusions in all 5 sections for each anchor, it is concluded that the T joints were probably welded very professionally, by a very highly skilled blacksmith who was able to avoid bulk defects in the forge-welding process. However, further work, including detailed CTs of both anchors followed by extended metallographic analysis of both anchors, may reveal more information and result in a better understanding of this behavior. The chemical etching that revealed the forge-welding lines, as shown in Fig. 14, suggests that the T-joints were welded not during consolidation of blooms, but rather after careful removal of the oxide film of the heated pieces, before hammering them together in a process that is not yet fully understood.

Taking into account the weights of the artifacts: 10.5 kg for Anchor A (20.4 ± 1.6 kg as reconstructed) and 20.6 kg for Anchor B (35.7 ± 3.2 kg as reconstructed), and the macro forge-weld lines on the surfaces of zones b, shown in Fig. 14, the following steps may be suggested for the manufacture of both anchors:

1. Anchor A was made from at least four pieces. The first part weighed about 10 kg, for the upper part of the shank (the part of the shank that was broken off and is now missing) and the other three weighed about 10.5 kg all together, for the perpendicular part (the artifact as is), two for the arms and one for the lower part of the shank (including the crown). The last three pieces were forged into their final shape in parallel. Anchor B was also made from at least four pieces. One weighed about 15 kg for the upper part of the shank and the other three weighed about 20.6 kg all together, for the perpendicular part as in Anchor A.
2. After forging the three pieces into their final shape, leaving a diagonal profile for both inner arms, they were forge-welded together by lap-joint welding. First, the right arm was put perpendicularly under the shank, leaving the crown projecting, and they were forge-welded together, as can be seen from line 2 in Figs. 14a and 11b of Anchor B, and from Fig.14c of Anchor A.
3. The left arm was put above the shank, the previously welded right arm, and they were forge-welded, as can be seen from line 1 in Fig. 14a and b of Anchor B, and from Fig.14c of Anchor A.
4. The first part was forged into a long shank, leaving a diagonal profile.
5. The “small shank anchor” was forge-welded to the rest of the shank.

It should be mentioned that the absence of forge-welding lines in Zone B for both anchors is very unusual because, practically, it is almost impossible to forge-weld two pieces without any oxidation of the surfaces (high temperature oxidation will cause the formation of new oxide layers again), or without using any fluxing agent, a process that must leave its “signature” in the forge-welding lines. Therefore, the reconstruction of the manufacturing process should be supported by the investigation of other iron anchor artifacts and

by further non-destructive radiographic test and destructive metallographic examinations of both Anchors A and B in a future work.

8. Conclusions

The two anchors discovered at the wreck site of *Tantura F* can be attributed to the ship. The metallurgical analysis of the iron anchors revealed the manufacturing processes and the metallurgical skills of the ancient smiths. The mechanical properties of the anchors were improved by several means:

1. The large amount of fuel placed into the furnace and the good tuyère arrangement, which contributed to the high carbon content of the raw material and, therefore, resulted in high hardness.
2. Decreasing the hardness of the raw material by a decarburization process might have occurred during prolonged heating before forge-welding, resulting in a decrease of hardness close to the surface, allowing good forge-welding and a very dense final product.
3. The *Tantura F* anchors had few forge-welding lines compared with the later anchors from Serçe Limanı.

The good mechanical properties of the anchors are also obvious, simply by the fact that they were found unbroken, except for the shank, and with significantly thick metallic core remains. The results of the chemical analysis, combined with the similarity in the production process of the two anchors, suggest that both were manufactured by the same process using the same ore.

The metallurgical information presented here broadens our understanding of the metallurgical evolution of iron anchors. It adds to the body of data collected so far, and adds parallels to the typology of iron anchors in the eastern Mediterranean during the early Islamic period. The simple methodology used here for obtaining the carbon content profile by microhardness test may be applied by others and provide important information.

Acknowledgments

This research was supported by Lord Jacobs of London, the Israel Science Foundation, the Hecht Foundation, Sir Maurice Hatter Fellowship for Maritime Studies and the University of Haifa, to which the authors are thankful.

The authors are grateful to Mr. Avshalom Zemer, Director of the National Maritime Museum in Haifa for his cooperation giving us access to the anchors and to Mr. Geyura Biraan for his enlightening comments. The authors would also like to thank Mr. Mario Levinstein from the School of Mechanical Engineering at Tel Aviv University for his assistance. Finally the authors would like to thank the two anonymous journal reviewers, both of which have spent much time and provided constructive and detailed feedback on the manuscript.

References

Barkai, O., Kahanov, Y., 2007. The Tantura F shipwreck, Israel. International Journal of Nautical Archaeology 36 (1), 21–31.
Barkai, O., Kahanov, Y., Avissar, M., 2010. The Tantura F shipwreck—the ceramic material. Levant 42 (1), 88–101.
Blakelock, E., Martinón-Torres, M., Veldhuijzen, H.A., Young, T., 2009. Slag inclusions in iron objects and the quest for provenance: an experiment and a case study. Journal of Archaeological Science 36, 1745–1757.
Beckmann, M., 1967. The Anchor. In: The Catholic Encyclopedia, vol. 1. Catholic University of America, Washington. 486.
Bhadeshia, H.K.D.H., 1985. Diffusional formation of ferrite in iron and its alloys. Progress in Material Science 29, 321–386.
Bonino, M., 1971. Ricerche sulla nave romana di Cervia, Atti del III Congresso Internazionale di Archeologia Sottomarina, Barcelona, 1961. Istituto Internazionale di Studi Liguri, Museo Bicknell, Bordighera, pp. 316–325.
Buchwald, V.F., 2005. Iron and Steel in Ancient Times. In: Historisk-filosofiske Skrifter, vol. 29. The Royal Danish Academy of Science and Letters, Copenhagen.
Buchwald, V.F., Wivel, H., 1998. Slag analysis as a method for the characterization and provenancing of ancient iron objects. Materials Characterization 40, 73–96.
Cabrera, C., 2007. Finds from Hispalis, A Byzantine anchor and medieval small boat from the ancient harbor of Seville. The INA Annual, 16–22.
Canarache, V., 1967. The Archaeological Museum of Constanta Muzeul Regionale de Arheologie Dobragea, Constanta.
Delwiche, D.E., 1982. Anchor metallurgy. In: Bass, G.F., Van Doorninck Jr., F.H. (Eds.), Yassi Ada Volume I: a Seventh-Century Byzantine Shipwreck. Texas A&M University Press, College Station, pp. 322–324.
Dillmann, P., L'Héritier, M., 2007. Slag inclusion analyses for studying ferrous alloys employed in French Medieval buildings: supply of materials and diffusion of smelting processes. Journal of Archaeological Science 34, 1810–1823.
Friede, H.M., 1979. Iron-smelting furnaces and metallurgical traditions of the South African Iron Age. Journal of the South African Institute of Mining and Metallurgy, 372–381.
Frost, H., 1963. From rope to chain. On the development of anchors in the Mediterranean. Mariner's Mirror 49 (1), 1–20.
Galili, E., Dahari, U., Sharvit, J., 1993. Underwater surveys and rescue excavations along the Israeli coast. International Journal of Nautical Archaeology 22 (1), 61–77.
Gargallo, P.N., 1961. Anchors in antiquity. Archaeology 14, 31–35.
Garagnani, G.L., Zucchi, F., Tommesani, L., Brunoro, G., 1996. Metallurgical investigations on 16th–17th century iron armours from the Museo Nazionale of Ravenna. Science and Technology for Cultural Heritage 5 (2), 83–94.
Green, J.N., 1973. An underwater archaeological survey of Cape Andreas, Cyprus, 1969–70, a Preliminary Report. In: Blackman, D.J. (ed.), Marine Archaeology, Proceedings of the Twenty-third Symposium of the Colston Research Society, held in the University of Bristol April 4th to 8th, 1971, London, pp. 141–79.
Günsenin, N., 2005. A 13th-century wine carrier: Çamalti Burnu, Turkey. In: Bass, G. (Ed.), Archaeology Beneath the Seven Seas. Thames and Hudson, London, pp. 118–123.
Haldane, D., 1990. Anchors in antiquity. Biblical Archaeology 51 (1), 19–24.
Harpster, M., 2005. A Re-assembly and reconstruction of the 9th-century AD vessel wrecked off the coast of Bozburun, Turkey, unpublished Ph.D. Dissertation, Texas A&M, College Station.
Hocker, F.M., Sara, W., Yamini, G.O., 1998a. The Byzantine shipwreck at Bozburun, Turky excavation: the 1997 Field season. INA Quarterly 25 (2), 12–17.
Hocker, F.M., Sara, W., Yamini, G.O., 1998b. Bozburun Byzantine shipwreck excavation: the final campaign, 1998. INA Quarterly 25 (4), 3–13.
Joncheray, J.-P., 1975. Une epave du Bas Empire: Dramont F. Cahiers D'Archéologie Subaquatique 4, 91–140.
Joncheray, J.-P., 1977. Mediterranean hull types compared. 2. Wreck F from Cape Dramont. International Journal of Nautical Archaeology 6 (1), 3–7.
Joncheray, J.-P., Brandon, C., 2007. L'Epave Sarrasine Agay A: Campagne 1996. Cahiers D'Archéologie Subaquatique 16, 223–249.
Kapitän, G., 1969–1971. Ancient anchors and lead plummets, Sefunim. Annual of the National Maritime Museum of Israel 3, 51–61.
Kapitän, G., 1973. Greco-Roman anchors and the evidence for the one-armed wooden anchor in antiquity. In: Blackman, D.J. (ed.), Marine Archaeology, Proceeding of the Twenty-third Symposium of the Colston research Society, held in the University of Bristol April 4th to 8th, 1971, London, pp. 383–395.
Kapitän, G., 1978. Exploration at Cape Graziano, Filicudi, Aeolian islands, 1977. International Journal of Nautical Archaeology 7, 269–277.
Kapitän, G., 1984. Ancient anchors – technology and classification. International Journal of Nautical Archaeology 13, 33–44.
Kemp, P., 1976. The Oxford Companion to Ships and the Sea. Oxford University Press, London.
Kingsley, S., Raveh, K., 1996. The Ancient Harbour and Anchorage at Dor, Israel: Results of Underwater Surveys 1976–1991. In: BAR International Series 626. Hadrian Books, Oxford.
Kocabaş, U., 2009. Camaltı Burnu I shipwreck. In: Bockius, R. (ed.), Between the Seas Transfer and Exchange in nautical Technology Proceedings of the Eleventh International Symposium on Boat and Ship Archaeology, 2006, Römisch-Germanisches Zentralmuseum, Mainz, pp. 227–237.
Marten, M., 2005. Spatial and temporal analysis of the harbor at Antiochia ad Cragum, unpublished M.A. Thesis, The Florida State university, College of Art and Sciences.
Martin, G., Saludes, J., 1966. Hallazgos arqueológicos submarinos en la zona de El Saler, (Valencia). Archivo de Prehistoria Levantina XI, 155–170.
Murray, W.M., Cliff, C.B., 1993. ASM Handbook. In: Welding, Brazing, and Soldering, second ed., vol. 6. ASM International, pp. 156–159.
Pollard, M., Batt, C., Stern, B., Young, S.M.M., 2007. Analytical Chemistry in Archaeology, pp. 47–48.
Pulak, C., 2007. The wrecks of Yenikapi the Gift of Storm. Arkeoatlas 6, 129–141.
Purpura, G., 1983. Il relitto bizantino di Cefalú. Sicilia Archeologica 51, 93–105.
Raveh, K., Kingsley, S.A., 1991. The status of Dor in Late Antiquity: a maritime perspective. The Biblical Archaeologist 54, 198–207.

Stech, T., Maddin, R., 2004. Iron analysis. In: Bass, G.F., Matthews, S.D., Steffy, J.R., Van Doorninck Jr., F.H. (Eds.), Serçe Limani an Eleventh-Century Shipwreck. The Ship and Its Anchorage, Crew, and Passengers, vol. I. Texas A&M University Press, College Station, pp. 192–195.
Tylecote, R.F., 1968. Solid Phase Welding of Metals. Edward Arnold, London.
Tylecote, R.F., 1992. A History of Metallurgy, second ed. The Metals Society, London.
Van Doorninck Jr., F.H., 1982. The anchors. In: Bass, G.F., Van Doorninck Jr., F.H. (Eds.), Yassi Ada. A Seventh-Century Byzantine Shipwreck, vol. I. Texas A&M University Press, College Station, pp. 121–141.
Van Doorninck Jr., F.H., 1984. The fabrication of some medieval iron anchors at the Bodrum museum in Turkey. In: Keith, D. (Ed.), Proceedings of the Thirteenth Conference on Underwater Archaeology. Fathom Eight Publications, San Marino, pp. 3–7.
Van Doorninck Jr., F.H., 2004. The anchors. In: Bass, G.F., Matthews, S.D., Steffy, J.R., Van Doorninck Jr., F.H. (Eds.), Serçe Limani an Eleventh-Century Shipwreck. The Ship and Its Anchorage, Crew, and Passengers, vol. I. Texas A&M University Press, College Station, pp. 189–233.
Visquis, A., 1973. Premier inventaire de mobilier de l'epave dite 'des jarres' a Agay. Cahiers d'archeologie subaquatique 2, 157–166.
Vrsalović, D., 1974. Istraživanja i zaštita podmorskih arheoloških spomenika u SR Hrvatskoj. Republički zavod za zaštitu spomenika kulture, Zagreb.
Wachsmann, S., Kahanov, Y., Hall, J., 1997. The Tantura B shipwreck: the 1996 INA/CMS joint Expedition to Tantura lagoon. INA Quarterly 24 (4), 3–15.
Wachsmann, S., Raveh, K., 1980. News: Israel, underwater work carried out by the Israel Department of Antiquities. International Journal of Nautical Archaeology 9 (3), 256–264.